Pocket Agent Devices for Personal Wireless Communications

Osamu Yuuki[†] , Kunihiro Yamada[‡] , Tadanori Mizuno[*, ***] ,
Hiroshi Mineno[**, ***] , Masakatsu Nishigaki[†, ***]

[†]Graduate School of Science and Technology, Shizuoka University, Shizuoka 432–8011, Japan
[‡]Professional Graduate School Embedded Technology, Tokai University, Tokyo 108–8619, Japan
[*]Faculty of Information Science, Aichi Institute of Technology, Toyota, Aichi 470–0392, Japan
[**]Faculty of Informatics, Shizuoka University, Shizuoka 432–8011, Japan
[***]Japan Science Technology and Agency, CREST, Chiyoda, Tokyo 102–0075, Japan
f5045016@ipc.shizuoka.ac.jp

***Abstract* –**There are many blind spots in the environment, where radio waves are attenuated. For example, the inside of a factory or tunnel can function as a blind spot for radio waves. Mobile phones or GPS devices are unable to successfully transmit or receive signals in such locations. We propose a new solution for such scenarios, where wireless telecommunication service is available in blind spots, using a "Pocket agent device". We have proposed various Pocket agent devices, each with their own advantages and disadvantages, which are summarized in this paper. For the purposes of developing a suitable agent device, we conducted experiments for characterization by path-loss models both indoors and outdoors. Statistical models were obtained where considerable measurement data was available. First, we considered the free-space path-loss model. The free-space path-loss model is adapted for the area between the transmitter and receiver that is free of obstacles. Next, we investigated the path loss exponent, which indicates how fast path loss increases with distance. We used the log-normal path-loss model here. Finally, we used this model to explore the available routes for communication. By using this method, an agent device is able to acquire a signal in a shorter time than when using alternative algorithms. This approach significantly increases the battery life of the device by reducing energy consumption.

Keywords: Pocket agent device, blind spot, wireless telecommunication, path loss, routing

1 INTRODUCTION

Today's world is dominated by ubiquitous computing [1] that is characterized by the marrying of computer power with everyday systems such a cellular phones, MP3 players and personal video, GPS, and radio frequency product identification and tracking systems. In recent years, a wide range of promising wireless communication protocols have emerged in many domains. For example, long-range wireless protocols, such as mobile worldwide interoperability for microwave access and high-speed downlink packet access, are essential for connection to the Internet, whereas short-range wireless protocols, such as IEEE 802.11, are used for mobile communications. In particular, hopping 802.11 networks are attractive solutions

for providing last-mile-hop broadband or wireless access in urban environments. Bluetooth are popular wireless protocols that permit connections among personal communication devices and consumer electronics, such as cellular phones and personal digital assistant devices.

On the other hand, the concept of mobile wireless sensor network in the context of pervasive ubiquitous networks has emerged in recent years, although Marc Weiser envisaged this concept as early as in 1991[1]. Networks of sensors based on networking technology [3] have built up in many cities. Such sensor networks are capable of being used to facilitate and extend crime prevention, security, environmental monitoring, agricultural products support, and so on. There are many static sensors and wireless communication spots in urban areas, making sensing and communications possible over a wide area. In such urban areas, emergency communication has become easy as a result of the spread of mobile communication devices.

However, it is not possible to foresee future disasters or accidents. There are many blind spots, such as in tunnels or buildings far from urban areas, inaccessible to radio waves required for communication; in these spots, there are not enough sensing devices or the necessary communication infrastructure to effectively handle emergency communications. In many cases, mobile devices are unable to communicate any information in such a zone. Bidirectional communications are important when a disaster or an accident occurs. For example, someone trapped in a tunnel cannot communicate with the outside world. He or she is instead forced to wait for a person passing through the tunnel.

In order to resolve the issue of communications blind spots, single-hop wireless networks based on a physical movable device are attractive solutions for providing last-one-hop broadband or wireless access in many environments. We have proposed various "Pocket agent devices". These devices are useful when in communications blind spots. There are advantages and disadvantages with each type of device. In this paper, these pros and cons are summarized.

There are some technical issues to be solved for the development of our proposed Pocket agent devices:

 (1) The device must be lightweight so that it can be carried easily. In this paper, we present lightweight functional devices. Then we compare the advantages and

disadvantages of four kinds of Pocket agent devices equipped with functional devices.

(2) It must be small in size. In this paper, we also discuss small functional devices.

(3) It should be battery powered, with enough battery life to perform effectively. In this experience, after the flight of the agent device using the proposed routing method, 87% of energy was preserved. The energy remaining in the agent device after flying was sufficient to perform bidirectional communication.

(4) As mobile technology matures, however, wireless networks are employed in more applications, and provide mobile users ubiquitous & continuous access to computing resources. Wireless networks are more prone to failures, and loss of access due to weak transmission power, terrain, interference, etc. Therefore, the reliability requirements of wireless networks should be rigorously assessed. Therefore, a spatial map of the local signal strength should be acquired for control of an agent device. We conducted RSSI measurement experiments in indoor and outdoor environments. We performed a simulation of the spatial map of the local signal strength.

(5) A mobile terminal has to determine the line-of-sight (LOS) of Agent device-to-Cellular phone station, Agent device-to-GPS satellites, and so on. In this paper, we assume that the nearby window in a room is the line-of-sight of radio waves. The window coordinates of the room are detected from an image by rapid object detection. In future, we will try to find the LOS by RSSI measurement. However, currently, the detailed positioning of base stations is not publicly disclosed by infrastructure companies, as this information could be used by rival companies to evaluate a region's market development.

For issues (1) and (2), ubiquitous computing aims at providing context-aware information services for individuals, anytime anywhere, by dint of ever-present computers and networks. Such computing devices will become very small in size. However, this paradigm shift in computing is not yet a reality for the general public due to a number of technical and social challenges [2]. We have therefore researched those communication devices and sensors that an individual can own. A user with a Pocket agent base device can use it for communications via other devices connected to the base device. We have conducted a feasibility study of Pocket agent devices using a variety of small & light devices. We summarize the main contributions of this paper as follows. In this paper, we focus mainly on issues (3), (4), and (5). The most profound technologies are those that weave themselves into the fabric of everyday life until they are indistinguishable from it [1]. In order to achieve this, the Pocket agent device should be able to act autonomously. We have driven the research in this direction by solving issues (3), (4), and (5). We measured path loss at the UHF band relevant to agent devices. We investigated how the path loss exponent indicates how fast path loss increases with distance. We used the log-normal path loss model in order to explore communication routes.

The rest of this paper is organized as follows. In section 2, we present related work that considers networks in disaster situations. Section 3 describes the concept of Pocket agent devices, and describes the architecture of these devices as designed by our researcher for wireless telecommunication in communications blind spots. Further, we analyze device architectures. Section 4 analyzes RSSI variability and routing of communications. Finally, our conclusions are given in Section 5.

2   RELATED WORK

First, we researched solutions of last-one-hop or multi-hop wireless communications. Micro strip reflect arrays convert a spherical wave produced by its feed into a plane wave through varying the structure and the dimensions of the reflect array elements. Predominantly, there are three versions of reflect array element structures including variable size patches, identical patch with variable length stubs, variable patch rotation angles. And the variable size patches method is the most popular way of varying the phase of the incident wave because of its simplicity. Micro strips reflect array is fixed to a base such as a building and is employed to reflect radio waves to a blind spot. Therefore, it cannot change the set location easily. On the other hand, the proposed Pocket agent device can move communication functional devices physically.

Figure 1 (a) shows the structure of crossed-dipole, the length of each square unit cell a is 5mm, the substrate thickness h is 0.508mm, the width of the crossed-dipole w is 0.4mm and the length of the crossed-dipole on the face of the substrate is L. Figure 1 (b) shows the reflection phase curve versus the length L of the crossed-dipole. The center frequency of the reflect array is 35GHz and the length of the square element is 5mm which is approximate 0.6 wavelengths at the center frequency [4].
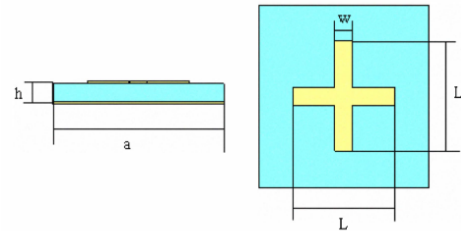
(a) structure of crossed-dipole
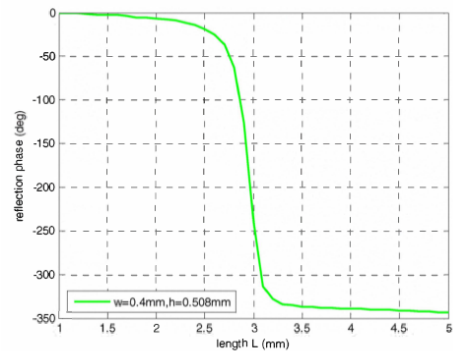
(b) phase response of crossed-dipole

Figure 1: Refract Array

The ballooned wireless ad hoc network has been proposed to ensure communication remains possible in a disaster situation [5]. Figure 2 shows a structure of ballooned wireless network node. A balloon utilize even though the disaster happened. The volume of balloon is 3.5 m^3 and filled up by helium gas which provides 28Kg as buoyancy. On the other hand, the total weight includes the balloon ($8.5\,kg$) and wireless access node ($8\,kg$) and the supporting ropes ($1.5\,kg$). Thus, the residual buoyancy is $10\,kg$ which is enough to keep the balloon 40-100 m high in the sky. The volume of this balloon is $3.5\,m^3$. The weight is $18\,kg$. These systems are intended to provide a communications infrastructure. As such, they are heavy and not feasible for personal use. The proposed Pocket agent device is small and light; therefore, it is portable and can be carried in the pocket.
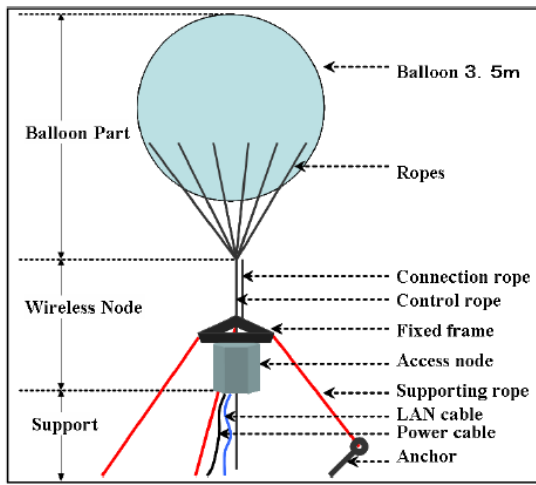

Figure 2: Balloon Network Node

VoIP using multi-hop 802.11 networks become attractive solutions for providing last-mile broadband access in urban environments. Voice over Internet Protocol (VoIP) over a wireless local area network (WLAN) is poised to become an important Internet application. However, two major technical problems that stand in the way are: 1) low VoIP capacity in WLAN and 2) unacceptable VoIP performance in the presence of coexisting traffic from other applications [6]. If there is no person around the user, communication is not possible. As for Pocket agent devices, personal communications are enabled in such conditions as well by moving communication functional devices physically.

Next, we describe studies of radio wave propagation. The free space propagation model is used to predict received signal strength when the transmitter and receiver have clear, unobstructed line-of-sight path between them. Satellite communication systems and microwave line-of-sight radio links typically undergo free space propagation. The electric wave which came out of the antenna will be decreased in the distant place, and will become weaker ,the received power of electric wave which is transmitted in free space, without any obstacle in circumferences, is expressed by Friis's transfer formula [7].

The received power: P_r is expressed by the following equation.

$$P_r = \frac{G_r \times P_t}{4 \times \pi \times d} \times \frac{\lambda^2 \times G_r}{4 \times \pi} = \left(\frac{\lambda}{4 \times \pi \times d}\right)^2 \times G_r \times G_t \times P_t \quad (1)$$

Where,
Transmitted electric power: P_t
Transmit and receive antenna gain: G_t, G_r
Received electric power: P_r
Propagation loss: L is expressed by the equation (2).

$$L = \left(\frac{4 \times \pi \times d}{\lambda}\right)^2 \quad (2)$$

Where,
Distance between transmission and reception: d, Wavelength: λ

The Friis free space model is only a valid predictor P_r for values of d which are in the far-field of the transmitting antenna. In mobile radio system, it is not uncommon to find that P_r may change by many orders of magnitude over a typical coverage area of several distances. The free-space loss model considers the area between the transmitter and receiver as an area free of obstacles that can absorb or reflect the transmitted energy, besides to consider the atmosphere perfectly uniform and no absorbent. However, in practice, this model is not accurate to describe the real behavior of the radio mobile channel [14] [15] [16] [17]. Therefore, it's necessary to modify this model in order to consider the complexity of the environment analyzed [13].

Next, we refer to Log-distance Path Loss Model [9].

Both theoretical and measurement-based propagation models indicate that average received power decrease logarithmically with distance, whether in outdoor or indoor radio channels. The average large-scale path loss for an arbitrary Transmitter-Receiver separation is expressed as a function of distance by using a path loss exponent n. $n = 2$ apply for free space, and n is generally higher for wireless channels. The log-distance path loss model presents by equation (3).

$$PL(d) = PL(d_0) + 10 \cdot n \cdot \log(d / d_0) \quad (3)$$

Where n is the path loss exponent which indicates the rate at which the path loss increases with distance, d_0 is the close-in reference distance which is determined from measurements close to the transmitter, and d is Transmitter-Receiver separation distance. The component $PL(d_0)$ is due to free space propagation from the transmitter to a 1 m reference distance (d_0).

Path loss - Link budget calculations require an estimate of the power level so that a signal-to-noise ratio or, similarly, a carrier-to-interference ratio may be computed [8]. Because mobile radio systems tend to be interference limited (due to other users sharing the same channel) rather than noise

limited, the thermal and man-made noise effects are often insignificant compared to the signal levels of co channel users. Thus, understanding the propagation mechanisms in wireless systems becomes important for not only predicting coverage to a particular mobile user, but also for predicting the interfering signals that user will experience from other RF sources.

Finally, we refer to log-normal path loss model [9].

The log-distance path loss model does not consider the fact that the surrounding environmental clutter may be vastly different at two different locations having same Transmitter-Receiver separation. This leads to measured signals which are vastly different than the average value predicted by equation (3). The log-normal path loss model presents by equation (4).

$$PL(d) = PL(d_0) + 10 \cdot n \cdot \log(d / d_0) + X_\sigma \qquad (4)$$

The term X_σ models the path loss variation across all locations at distance d from the source due to shadowing, a term that encompasses signal strength variations due to artifacts in the environment (i.e., occlusions, reflections, etc.). Accordingly, received signal strengths at locations that are of equal distance from the transmitter are considered normal random variables. The term $PL(d_0)$ simply gives

PL at a known close in reference distance do which is in the far field of the transmitting antenna (typically 1 km for large urban mobile systems, 100 m for microcell systems, and 1 m for indoor systems) and X, denotes a zero mean Gaussian random variable (with units of dB) that reflects the variation in average received power that naturally Occurs when a PL model of this type is used. Since the PL model only accounts for the distance which separates the transmitter and receiver, and not any of the physical features of the propagation environment, it is natural for several measurements to have the same Transmitter-Receiver separation, but to have widely varying PL values. This is due to the fact that shadowing may occur at some locations and not others, etc. While accounts for signal variations over large scales, the received signal strength can vary considerably over small distances (in the order of wave length) and small time scales, due to multipath fading [10]. As a result, packet loss can exhibit wide variations even when d changes. Indoor RF signal propagation models, including models that take into account the number, delay, and power of indoor multipath components [11]. This model can be used over large and small distances [12], while empirical studies have shown that it can effectively model multipath indoor channels. There has been a study of implications of the log-normal path loss model [18] [19]. The approach significantly increase the lifetime of the system by conserving energy that the sensing nodes otherwise would use for communication [20]. And, Efficient Receiver-Initiated Link Layer for Low-Power Wireless has been described [21].

We proposed the direct-routing algorithm by using log-normal path-loss model. This method is faster than other algorithms, and as such, it will reduce the energy consumption of devices that use it.

3   CONCEPT OF PROPOSED DEVICES

3.1   Concept of Pocket Agent Device

As shown Fig. 3, there is a high possibility that radio waves are intercepted inside a tunnel, which is surrounded by thick concrete. We call such a spot a "radio blind spot." Wireless devices in a radio blind spot cannot communicate with those that are outside the tunnel, as shown in Fig. 4. The concept of routing using a Pocket agent device is shown in Fig. 5. The inside of a tunnel surrounded by thick concrete is in most cases opaque to the radio waves required for wireless communication. We call such a zone a communications blind spot. This blind spot is shown as the area surrounded by the dotted line in Fig. 5.

We describe the workflow of the service below.

A Pocket agent device is equipped with a GPS receiver or mobile Wi-Fi router. Therefore, in a communications blind spot, such a device needs to move to an exit, or a nearby window, in order to receive a satellite signal or cellular phone signal. As shown in Fig. 5, a sensing device, such as a Bluetooth GPS, and a wireless router, such as a mobile Wi-Fi router, are moved to the exterior of a communications blind spot. In this way, the receiving and transmitting functions of these devices are recovered.

After that, the portable device equipped with Bluetooth and Wi-Fi communicates with an external sensing device and wireless router. Bidirectional communications thus become possible from a communications blind spot.
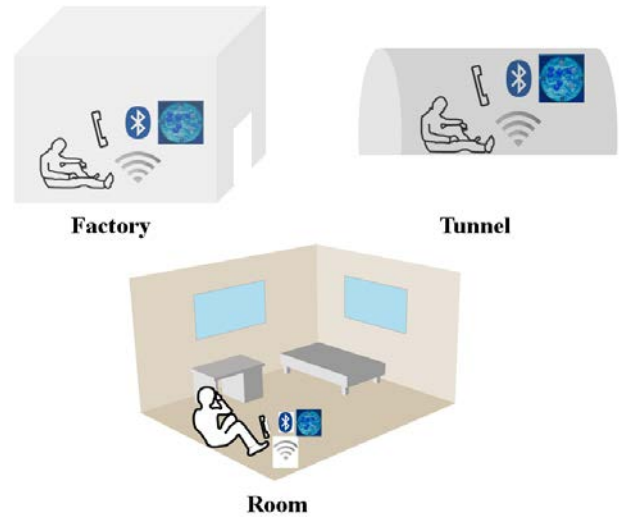

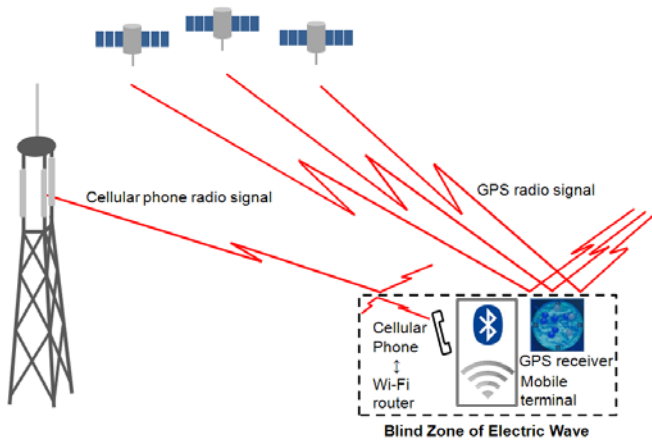Figure 3: Various blind spots.

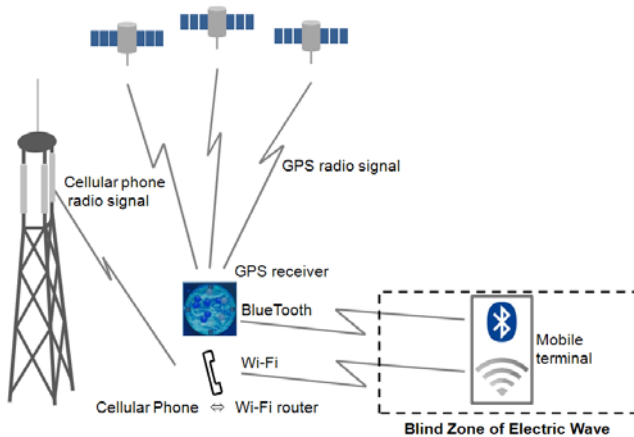Figure 4: Communications in a blind spot.

Figure 5:
Pathway of the proposed communication
in a communications blind spot.

The scenario is shown in Fig 6. We prepare a mobile terminal in a communications blind spot. We then measure the received signal strength indication (RSSI) of the line. We calculate the RSSI map around the device along with the path-loss variations. An RSSI map is made from the values experienced by the mobile terminal. The communication path is then explored. The route to the target point can be calculated from the RSSI map. We can decide upon the target point. As the agent device moves, so too does this point. We finally establish a communication path. The agent device communicates bidirectional. We can receive positional information through GPS. We can then send the message along with positional information to a terminal at another location.
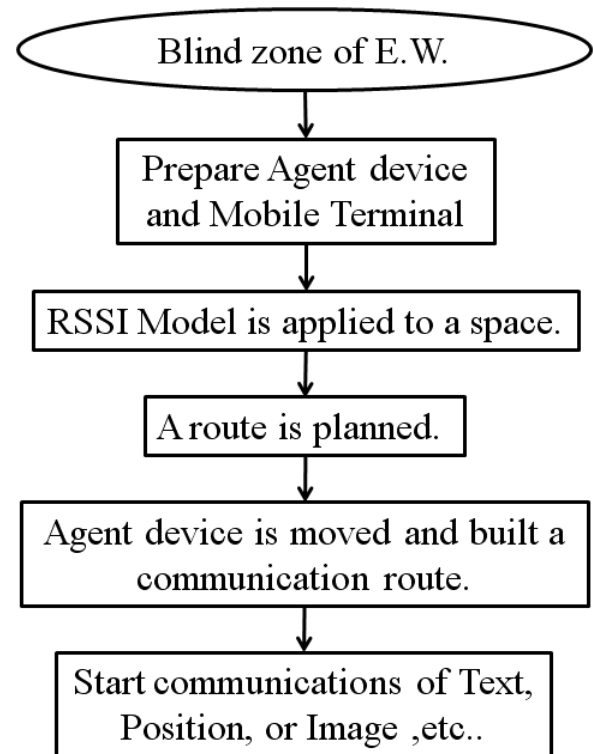
Figure 6: Scenario in a communications blind spot.

3.2 Architectures of Pocket Agent Devices

We have so far considered various agent devices. We show the devices in Figs. 7 - 10.

(1) Pocket Agent Device: Ball Type
The structure of an agent base device in the form of a ball is shown in Fig. 7 (c).
The ball form of the Pocket agent device is equipped with a sensing device, such as a Bluetooth GPS (a) [26], a router, such as a mobile Wi-Fi router (b) [27], and so on. In order to absorb collision shocks, these devices are wrapped with low-rebounding rubber or low-repellence urethane foam.
Furthermore, the low-rebounding rubber or low-repellence urethane foam is covered with synthetic rubber [22].
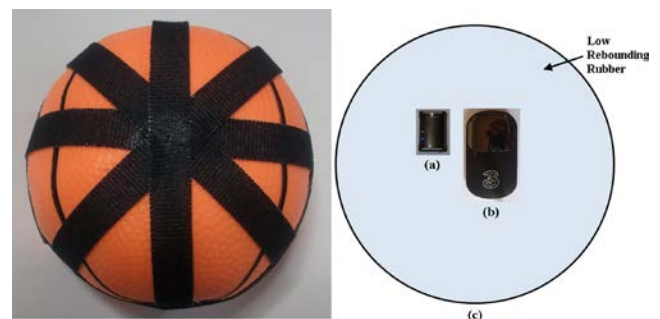

Figure 7: Parts of Pocket agent device.
(a) GPS; (b) Mobile Wi-Fi Router,
(c) Pocket agent base device [Ball Type]

(2) Pocket Agent Device of Vehicle Type

An agent base device in the form of a vehicle, as shown in Fig. 8 (c), is equipped with a sensing device, such as a Bluetooth GPS (a) [26], a router, such as a mobile Wi-Fi router (b) [27], and so on.

The vehicle form of the Pocket agent device constructs a communications path by moving on the ground in a communications blind spot [23].
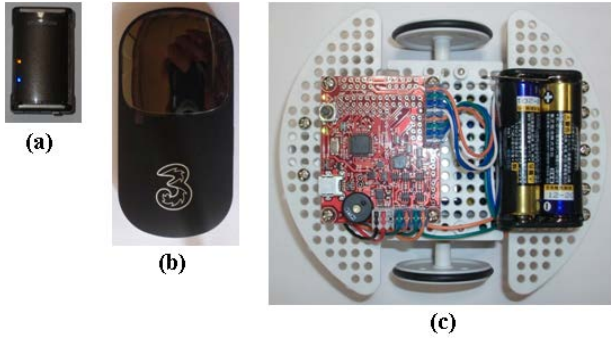

Figure 8: Parts of the Pocket agent device.
(a) GPS; (b) Mobile Wi-Fi Router,
(c) Pocket agent base device [Vehicle Type]

(3) Agent Device: Flyer Type

An agent device in the form of a flying machine is shown in Fig. 9 (c). This type of agent base device is equipped with a sensing device, such as a Bluetooth GPS (a) [26], a router, such as a mobile Wi-Fi router (b) [27], and so on.

Constructing a communications path through the agent device is possible even if there is an obstacle on the ground or in the path of any communications signals [24].
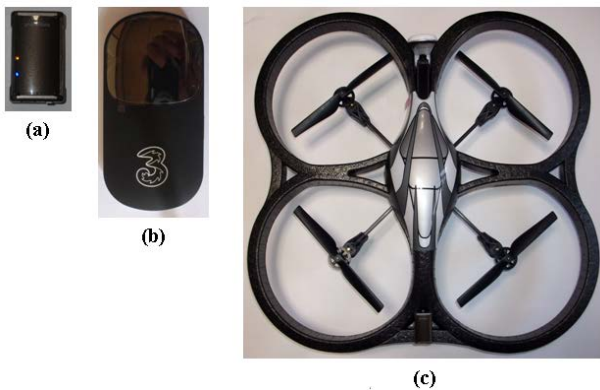

Figure 9: Parts of the agent device.
(a) GPS; (b) Mobile Wi-Fi Router,
(c) Agent base device [Flyer Type]

(4) Agent Device: Robot Type

An agent base device in the form of a robot is shown in Fig. 10 (c). The agent device is equipped with a sensing device, such as a Bluetooth GPS (a) [26], a router, such as a mobile Wi-Fi router (b) [27], and so on. The agent device constructs a communications path from a communications blind spot to a zone where communications are possible by autonomously searching the RSSI using the RSSI receiver. Once a path is established, it enables bidirectional telecommunications [25]

Figure 10: Parts of the agent device.
(a) GPS; (b) Mobile Wi-Fi Router,
(c) Agent base device [T Robot Type]

3.3 Comparison of Four kinds of Pocket Agent Devices

We compared the advantages and disadvantages of the various Pocket agent devices. Our findings are summarized in Table 1. Sometimes, there is an LOS at a high altitude such as a high window and the top of a building. Flyer type can reach the LOS. If the obstacles are spread on the ground, the flyer type can fly over the obstacles. Therefore, the flyer type has many advantages in different cases. We want to encourage the development of the flyer type.

Table.1 Comparison of Pocket Agent Devices.

Operating Conditions	Construction of Agent Devices	Advantages	Disadvantages
Road, High Windows	 Ball Type	①Cheap (≒12 ,000 yen) ②Easy to carry. (≒12cm, 214g) (GPS:44×112×57, 18g) (Router:86×46.5×10.5, 90g) ③Is inflammable. (No electric parts on the surface) ④Can, if wrapped in adhesives, adhere to, e.g., high windows.	①May roll too much when thrown. ②Throwing ability is required.
Flat Road	 Vehicle Type	①Comparatively Cheap (≒17,000 yen) ②Easy to carry. (≒13cm, 308g) (GPS:44×112×57, 18g) (Router:86×46.5×10.5, 90g) ③Is stable.	①A route plan is required. ②Unable to move past obstacles.
Obstacle on a Road, High Windows	 Flyer Type	①High flexibility of movement. (Movable to X, Y, and Z directions) (≒11.5cm, 47g: Only the base device of the flyer)	①Additional weight of a launcher is required.($\leqq$10g) ②Flight control is difficult.(gyro, acceleration sense, image recognition etc.) ③It is difficult to carry. ④It is relatively expensive. (≒20,000 yen)
Road	 Robot Type	①Autonomous movement is possible. "Walking in a confined area", "Walking on uneven surface", "tipping-over control", "getting up from a fallen position" and "human-interactive operations in open spaces" (20 degree of freedom, 2-axes gyro, 3-axes velocity sensor, 3-axes force sensors, and CPU + motion planning) ②Can be installed in communications blind spots, and can move autonomously to detect communications paths. (RSSI measurement + motion planning) ③Highly compact electrical system packaging (Height: 37cm, Weight: 1.5kg)	①It is relatively expensive. (≒510,000 yen)

4   PROOF OF CONCEPT

4.1   Indoor Testing Environment

We conducted RSSI-measurement experiments in the room of a building in an urban area. The relation between a transmitter (Pocket WiFi) and receiver (Wireless LAN adapter) is shown in Fig. 11. For every measurement, the height of the transmitter was moved by 20 cm for the x and y coordinates, from 0 cm to 160 cm.
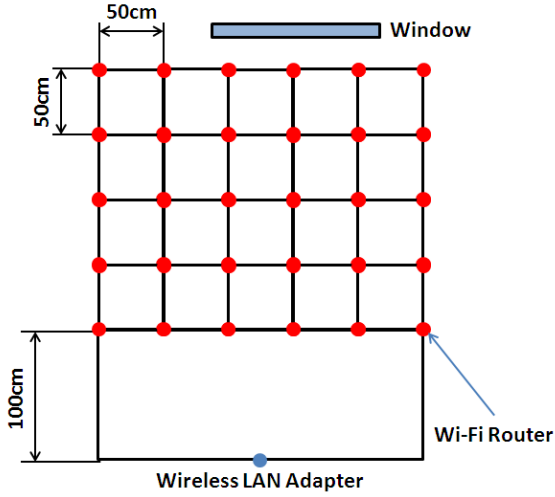

Figure11: Positioning of transmitter and receiver.

Radio waves in the room in the industrial, scientific, and medical (ISM) bands are shown in Fig. 12. About 17 waves were simultaneously received by the wireless LAN adapter. As such, we assumed that there was substantial interference in the room.

Figure12: RSSI in the ISM bands in the room.

4.2   Indoor propagation experiments

We measured 300 points of RSSI data per place in the room. We show data of mid row points in Fig. 13. The approximation lines are presented by equation (4). While n is 2 for free space, but is generally higher for wireless channels.

The component PL0 is due to free space propagation from the transmitter to a 1 m reference distance. And Xσ denotes a zero mean Gaussian random variable that reflects the

variation in average received power that naturally Occurs when a PL model of this type is used. Since the PL model only accounts for the distance which separates the transmitter and receiver, and not any of the physical features of the propagation environment, it is natural for several measurements to have the same Transmitter-Receive separation, but to have widely varying PL values. The term Xσ models the path loss variation across all locations at distance d from the source due to shadowing; the term that encompasses signal strength variations due to artifacts in the environment (i.e., occlusions, reflections, etc.). Multipath delay spread Time dispersion varies widely in a mobile radio channel due to the fact that reflections and scattering occur at seemingly random locations, and the resulting multipath channel response appears random, as well.

The received signal strength can vary considerably over small distances due to multipath fading. As a result, packet loss can exhibit wide variations even when d changes. Indoor RF signal propagation models are influenced from the amount of number, delay, and power of indoor multipath components.

We employ the popular log-normal path-loss model. This model can be used over large and small distances, and empirical studies have shown that it can effectively model multipath indoor channels. We investigated the implications of the log-normal path-loss model on deploying and moving an agent device. The measured RSSI values vary according to the surrounding physical environment. For example, the received signal strength y at 80 cm height is expressed in equation (5).

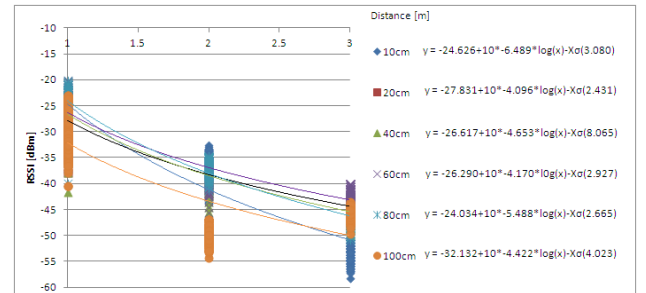$$y = -24.034 + 10 \times (-5.488) \times \log(d/d_0) + x_{\sigma(2.665)} \quad (5)$$

Figure13: RSSI in the room

4.3   Indoor Experiments & Results

First, we simulated RSSI in the room. We used the log-distance path-loss model for the simulation. We used equation (5) without the path-loss variation (term X_σ) to calculate the 3D distribution of RSSI in the room.

The RSSI values are shown in Fig. 14. The PL model only accounts for the distance which separates the transmitter and receiver, and not any of the physical features of the propagation environment; it is natural for several

measurements to have the same Transmitter-Receiver separation, but to have widely varying PL values.
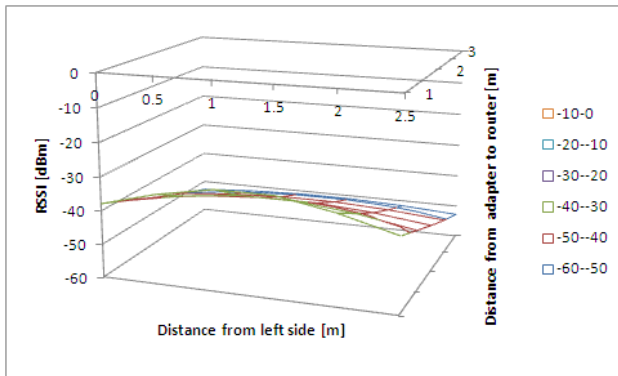

Figure14: The distribution of RSSI by the simulation (without Gaussian noise).

Next, we simulated RSSI with the log-distance path-loss model with log-normal shadowing. We used equation (5) for the simulation. This equation contains the Gaussian distribution term. The model gives a similar result to the measured RSSI. We show the results in Fig. 15.
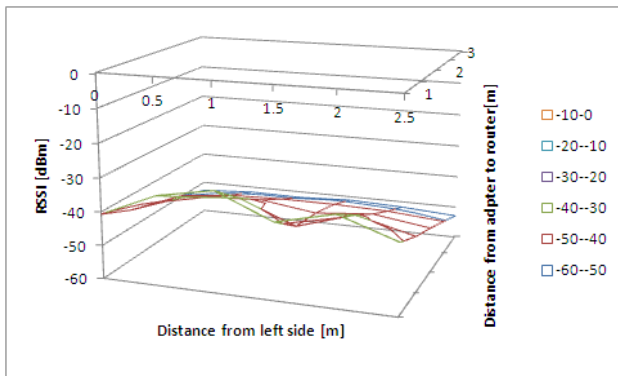

Figure15: The distribution of RSSI with Gaussian noise by the simulation (with Gaussian noise)

Finally, we measured the 3D distribution of RSSI in the room. The measured RSSI values are shown in Fig. 16. The measured values contain more variations than the simulated values, due to the number of other radio waves detected in the room. These waves were received by the wireless LAN adapter. Some values do not match the values expected from a Gaussian distribution. However, the map derived from the measured values showed the same tendency as the map derived from the simulation values. Therefore, we assume that the log-normal path-loss model can be used to explore communications routes.
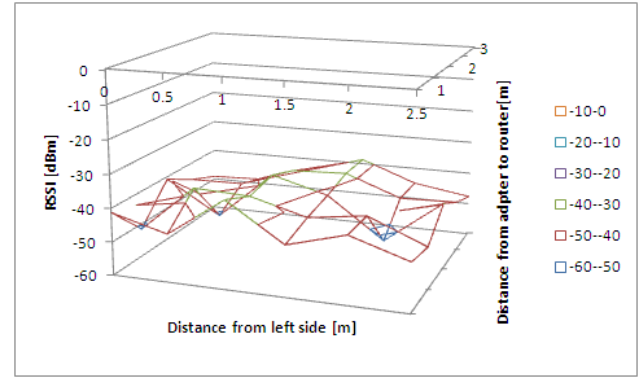

Figure16: The RSSI measured in the room

4.4 Search of the Route of Communications Using the Log-Normal Path Loss Model

We investigated the communications path between a Pocket WiFi device and a wireless LAN. We show cells of transmitters in Fig. 17. The positions of transmitter and receiver are shown in Fig. 11.
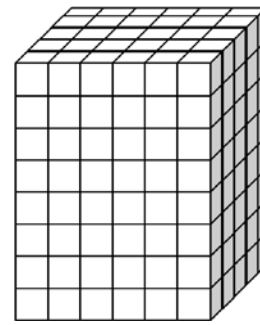

Figure17: The cells of transmitters

The agent device, represented as a transmitter in this case, searches the appropriate RSSI in order to communicate with the receiver. While an agent device in our proposed system may use both a wireless LAN and cellular phone network, the agent device should search for an equal or stronger RSSI position that is able to communicate with the mobile terminal. The target cell is shown as a red circle in Fig. 18. As shown in Fig. 11, there is a window near the cell in order to communicate with GPS or cellular phone networks. As shown in Fig. 1, the agent device is equipped with a GPS receiver and/or mobile Wi-Fi router. As such, an agent device may need to be moved to a nearby window in order to receive a satellite signal or a cellular phone signal. The target cell should match to the above-mentioned RSSI conditions. Moreover, the RSSI is expected to be stronger than -90 dBm. Figure 18 shows the basic method for routing. The route may pass through all the cells in a box. A box has 240 cells. We show the path that passes through a cell as a gray circle in Fig. 18. Equation (6) presents the number of possible routes from a source cell to a target cell. And, Equation (7) presents the time complexity of the algorithm in the worst case.

$$G_n = (n-1)! \tag{6}$$

Where, $n = 240$, $\therefore D_n = 1.695E + 466$

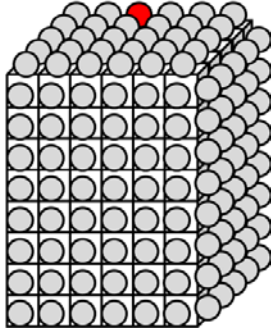$$N = O\left(n^{240}\right) \tag{7}$$

Figure18: Method 1: Search of all transmitter cells.

An agent device should reach the target cell as quickly as possible. If it takes a long time to reach the target cell, the agent device will use more (and potentially all) the battery energy. An agent device should reduce its energy consumption by using the other algorithms. We have to search for a shorter path to reach the target cell for an agent device. Dijkstra's algorithm can be used for this purpose. Equation (8) presents the number of possible routes moving from a starting cell to a target cell And, Equation (9) presents the time complexity of the algorithm.

$$D_n = \frac{1}{2} \times n \times (n-1) \tag{8}$$

Where, $n = 240$, $\therefore D_n = 28,680$

$$N = O\left(n^2\right) \tag{9}$$

We show Dijkstra's algorithm in Fig. 19. An agent device can find the shorter route. An agent device tries to pass D_n routes in a box by Dijkstra's algorithm. The route is shown with the line in Fig. 19.
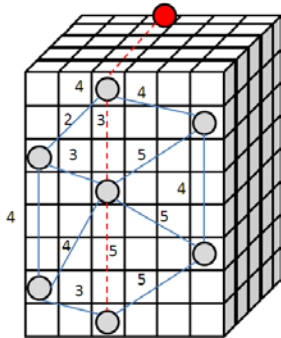

Figure19: Method 2:
Search by Dijkstra's Algorithm

We also propose a direct-routing algorithm to further decrease the time it takes for an agent device to reach the target cell.

$$DI_n = 1 \pm \alpha \tag{10}$$

$$N = O(1) \tag{11}$$

We show the behavior of the proposed algorithm in Fig. 20. We can decide upon the target cell by using the log-normal path-loss model. The route is then connected directly to the target cell. The route is shown with the blue line in Fig. 20. The route takes only one path in the box. Some simulation values may not match to the actual measurement values; in rare cases, an agent device may have to find the cells around the target cell by trial and error. The numbers of trial-and-error routes are presented as term α in equation (10). And, Equation (11) presents the time complexity of an algorithm.
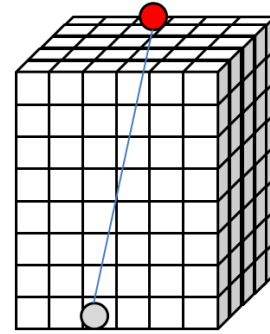

Figure20: Method 3:
Search by predicting signal attenuation

4.5   Outdoor Testing Environment

We evaluated RSSI and broadband speed around the communications blind spots. There are many tunnels in Kanagawa prefecture that are around 200 m in length. We conducted the experiments in these tunnels, using them as the communications blind spots. There is a roughly 1.5 m width sidewalk in the tunnels. Dense forest surrounds each of the selected tunnels.

The positions of these tunnels on Google Maps [28] are shown in Fig. 21.

Figure21: Tunnel locations for the experiment.

The specifications of the tunnels are shown in Table 2.

Table2 Tunnels' Specifications.

Tunnel name	AIKAWA	OOSAWA	RYOUMUKAI
Length	146m	223m	233m
Width	9.75m	9.25m	9.25m
Hight	4.50m	4.50m	4.50m

Figures 22, 23, and 24 show photographs of the tunnels.

Figure22: Picture of RSSI experiment in AIkawa tunnel

Figure23: Picture of RSSI experiment in Oosawa tunnel

Figure24:
Picture of RSSI experiment in Ryoumukai tunnel

4.6 Outdoor propagation Experiments

Although dependent on the position of each satellite at the time, the GPS radio signal from a satellite near its zenith will be intercepted by the outer wall of a tunnel. If a device tries to derive its position from the signal of three or more sets of satellites inside a tunnel, it is difficult to receive the signals of all satellites simultaneously.

On the other hand, the visual angle of the transmitting point of the base station from the inside of a tunnel is used for the calculation of distance which the direct wave of mobile phones, such as 3G Cellular phone signal, reaches into a tunnel. Calculation is possible by equation (9). (It is also possible in buildings such as factories to calculate the range of radio waves from the height of the opening of an entrance using the same equation.) The figure containing the parameter for calculation is shown in Fig. 25.

The distance from a base station to a tunnel's entrance is expressed by the following equation (12).

$$a = \frac{h_t}{\tan \Theta} \qquad (12)$$

Here,

a : The direct radio-wave range from the tunnel entrance.

h_t : The tunnel height.

Θ : The visual angle that the extension line from a base station antenna to the exit edge of a tunnel makes from a road surface..

Pr (RSSI) is approximated by equation (13).

$$\mathrm{Pr} = P_0 - 10 \cdot n \cdot \log(d / d_0) \qquad (13)$$

Here,

Pr : Received power at a distance d

P_0 : Power received at close-in reference point

d : Distance of separation between a transmitter and receiver

d_0 : Reference point at small distance

The base station is architected with the cell or sector composition. The range of radio waves in a tunnel changes according to these architectures and the numbers of base stations. These compositional differences influence the signal-to-interference ratio [9]. Furthermore, the received power is influenced by multi-path fading that result from the reflections from a wet road surface. The distance calculated by the equation is therefore a rough value. Additionally, the positioning of base stations is not publicly disclosed by infrastructure companies, as this information could be used by rival companies to evaluate a region's market development. Therefore, due to the lack of information about the positioning of base stations, we research the RSSI in tunnels. We then propose an alternative solution to the problem in Chapter 4.8.

The range of Class 1 Bluetooth transmissions is about 100 m. The range of a Wi-Fi standard broadcast is also about 100 m. Therefore, a tunnel with a length of up to 200 m can be covered by choosing the exit that is nearer to the person inside the tunnel. It is presumed that the 100 m range is also a practical communication distance in a building like a factory. The area of "the productive facility, the green tract of land, and the environmental facility" is defined by the use of the space beyond a fixed scale (e.g., the sum total of plottage is 9,000 m^2 or more, or building area is 3,000 m^2 or more) in Japan. Therefore, the longest diagonals of many factories are presumed to be 100 m or less.
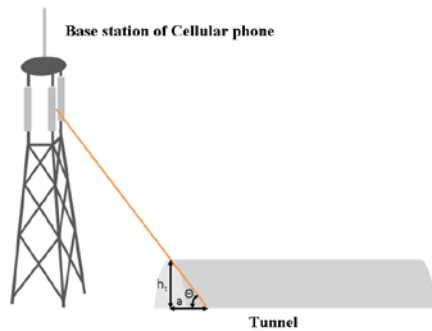
Figure 25: The range of access of
the direct cellular phone signal in a tunnel.

4.7 Outdoor Experiments & Results

We measured the RSSI using Pocket WiFi [29]. The RSSI outside a tunnel is shown in Fig. 26 (a). Communication by 3G Cellular phone signal is available here. The RSSI inside a tunnel is shown in Fig. 26 (b). In this case, communication by 3G Cellular phone signal is not available. The display of Pocket WiFi shows "No Service".
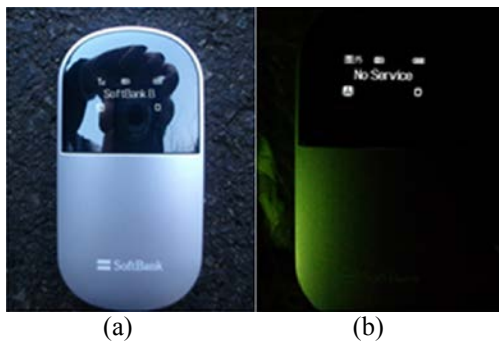

Figure 26:
Cellular phone signal conditions.
(a) Outside of a tunnel;, (b) Inside of a tunnel

We measured the GPS signal strength. The signal strength outside a tunnel is shown in Fig. 27 (a). The positioning by GPS signal is available here. The RSSI inside a tunnel is shown in Fig. 27 (b). The positioning by GPS signal is not available here. The display shows that the entire satellite signal is 0.

Figure 27: GPS signal conditions.
(a) Outside of a tunnel;, (b) Inside of a tunnel

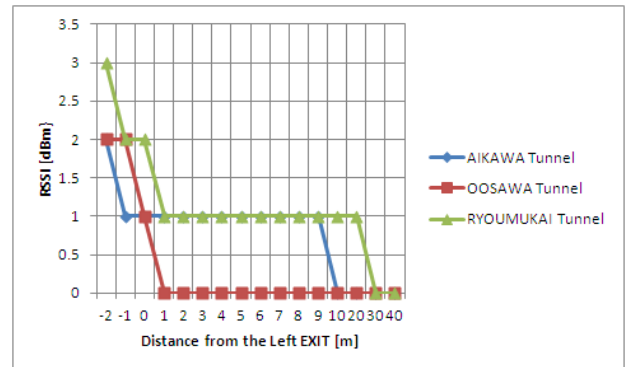We measured the RSSI in three tunnels. The RSSI of the left-side exit is shown in Fig. 28.

Figure28: RSSI in the tunnels (left-side exit)

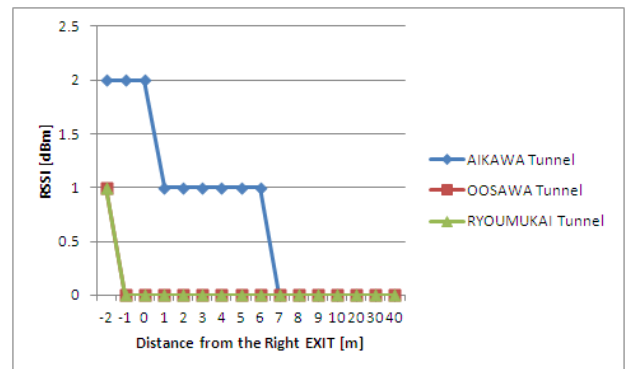The RSSI of the right- side exit is shown in Fig. 29.

Figure29: RSSI in the tunnels (right-side Exit)

The RSSI of the right-side exits of Oosawa and Ryoumukai tunnell is poor due to the circumference of the exits being surrounded by mountains. The environment around the right-side exit of the Oosawa tunnel is shown in Fig. 30. (The tunnel in the photograph is another tunnel.) The difference of the RSSI value is caused by these geometrical features.

Figure30:
Photograph of the right-side exit of Oosawa tunnel

We set Pocket WiFi at the exit of the tunnel (i.e., at 0 m), and measured the RSSI from inside the tunnel.
The RSSI values show the tendency of free-space path-loss model, as shown in Fig. 31.
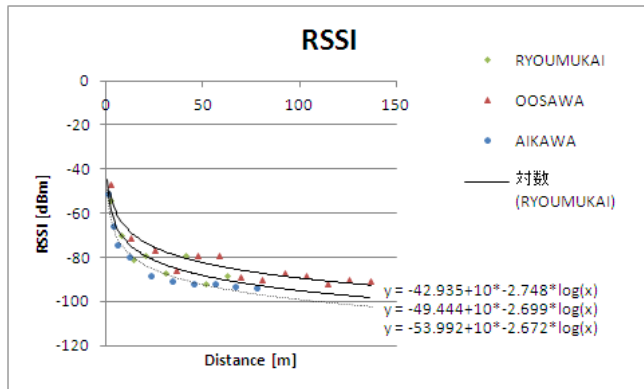
Figure31: RSSI in the tunnels

Next, we confirmed RSSI and broadband speed for the different types of device.

The models used for the experiment are shown in Fig. 32.

The ball-type agent device is equipped with Pocket WiFi. Pocket WiFi is put in the ball as shown in Fig. 32 (a).

Pocket WiFi for the vehicle form was placed on the ground as shown in Fig. 32 (b).

The flyer type's Pocket WiFi was installed at a height of 1 m from the ground as shown in Fig. 32 (c).

There are two communication methods for the flyer-type agent device: one where communication starts after the agent device lands on the ground, and the other, where communication starts during the flight. In the case of the former, its effectiveness is near equal to the value measured by the model of 32 (b), and, in the case of the latter, it is near equal to the value measured by the model of 32 (c).

The Pocket WiFi for the robot type is put in a box as shown in Fig. 32 (d).
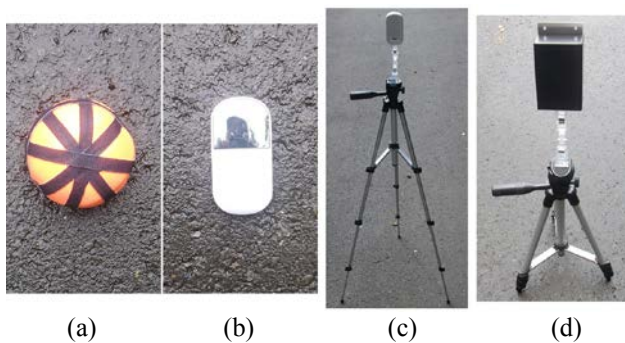

(a)   (b)   (c)   (d)

Figure32: The four kinds of simulation model.

SIDDR [31] was used for the measurement of RSSI.

Broadband Speed Test [32] was used for the measurement of the broadband transmission speed.

The screen of measurement results of RSSI and broadband speed is shown in Fig. 33.

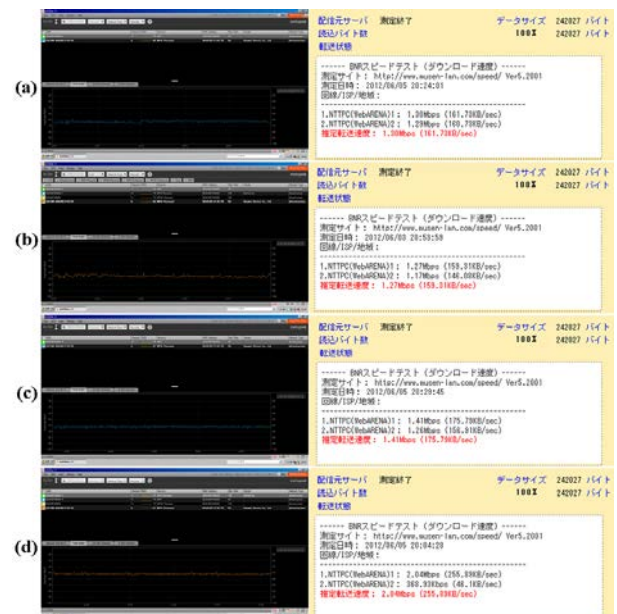In this experiment, the AC/DC adaptor was used for the power supply of the Wi-Fi router.

Figure33: RSSI level and Broadband speed

Figure 34 shows the RSSI of the four kinds of simulation model.

Since the RSSI of type (a) is surrounded by low-repellence urethane, the RSSI is weaker than for type (b). The RSSI of type (c) is stronger than that of type (b), and the RSSI of type (4) is the strongest of the models. This results from the reflection of radio waves from the metal surface of the case. At the result, the RSSI goes up.
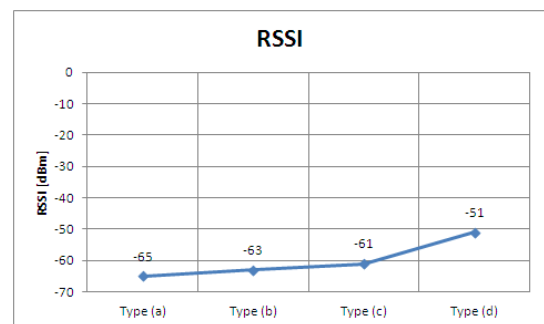

Figure34:
RSSI of the four kinds of simulation models

The measurement result of the broadband speed is shown in Fig. 35. The RSSI and the speed are correlated with each other. Although we believe that the relationship between type (a) and type (b) is the opposite, we assume that the difference of these values is within the range of the measurements' error. The similarities of RSSI and broadband speed are related to the architectures.

At the result of this experiment,

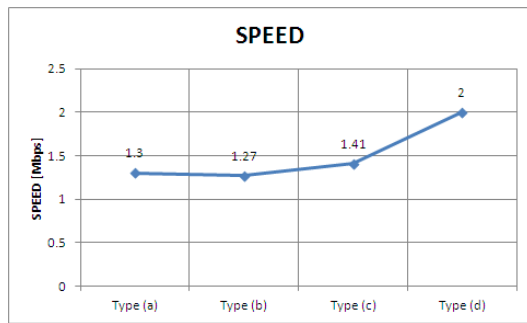Type (d) > Type (c) > Type (a) > Type (b)

Figure35:
Broadband speeds of the four kinds of Simulation models.

4.8   Controlling the Agent Device

We conducted the experiment with the flyer-type agent device. The control flow is shown in Fig 36. We prepared a mobile terminal and a program in the mobile terminal. We used the Eee-PC 900A with an 8.9 inch display [30] as a mobile terminal in this experiment (an iPhone or other smart-phone, or an iPod could also be used). The agent device is equipped with the photoMate Mini GPS Recorder 887 [26], Pocket WiFi C01HW [29], and a built-in camera. We measured the RSSI of one line. We show the RSSI in Fig. 39. This program calculates the RSSI map around the person, along with the path-loss variations. We show the RSSI map in Fig. 40. A RSSI map is made from data measured by the mobile terminal.

We operated programs for the measurement of RSSI, extraction of RSSI from the image, mapping the data in 3D, display of the map in the window, and the controlling of Agent device. We programmed this agent device with the following control sequence. First, the agent device moves forward after taking off perpendicularly. Next, the agent device moves to the right or the left. This moving sequence takes three steps, although it should be noted that the steps are fewer than required with other algorithms.
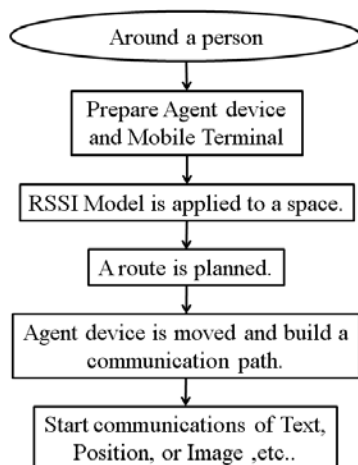

Figure 36: The control flow.

We show a more detailed control flow chart in Fig. 37.
(a) Main flow: The detailed control flow that used the path loss model between an agent device and a LAN adapter is

shown in Fig. 37 (a). The agent device is equipped with a wireless router with a cellular phone line, and GPS. First, it is determined whether the line-of-sight of an electric wave is effective between a mobile terminal and an agent device. The mobile terminal judges whether the characteristic of the radio wave propagation is similar in the case of free spaces, or is being influenced by shadowing, multi-pass fading, etc. If it is in a free space outdoor environment, it is possible to use the log-distance path loss model that assumes that n is two. However, at the place where it is easy to receive interference such as shadowing and/or multi-pass fading as in urban areas, then since RSSI is varied, the log-distance path loss model cannot be used in its original form. In this case, the RSSI between a mobile terminal and an agent should be measured only once. It is more desirable to be able to carry out a real-time operation by using the log-distance path loss model in case of outdoor environments. Users rarely visit the same outdoor place repeatedly. The log-distance path loss model is memorized at a mobile terminal. Users in urban areas typically spend more time indoors for habitation, work, etc.; therefore, it is comparatively easy to measure the RSSI in indoor environments only once. In this case, the parameter that serves as a variation factor from an actual measurement is memorized at a mobile terminal. The mobile terminal calculates the distance from itself to the agent device. The parameter is use for model fitting. Then, an RSSI space map is simulated using these results. These processes are performed as a batch process. Once it memorizes what was surveyed, the mobile terminal and the agent device use the map for a real-time operation. Next, the LOS of the electric wave between the agent device and a cellular phone base station, or a GPS is detected. Data from both sides determine the migratory pathway of an agent device. Once it memorizes what was surveyed, a real-time operation uses the map for driving the agent device. The migratory pathway of the agent device is determined from the RSSI data obtained from both sides. Moving an agent device in accordance with this course is controlled by using the API. Next, each predefined process is described.

(b) RSSI measurement predefined process Fig. 35 (b) is a flow of measurement of the RSSI between the mobile terminal and the agent device. The RSSI between a mobile terminal and an agent is measured by batch processing only once. Real-time measurement is also possible. However, the agent device should move many points to measure the RSSI, leading to wastage of electric power. The n parameter is calculated using the RSSI by the mobile terminal. Next, the standard deviation for the curve is obtained using actual measurement data and the log-distance path loss model. The n parameter and standard deviation are stored in the memory of the mobile terminal.
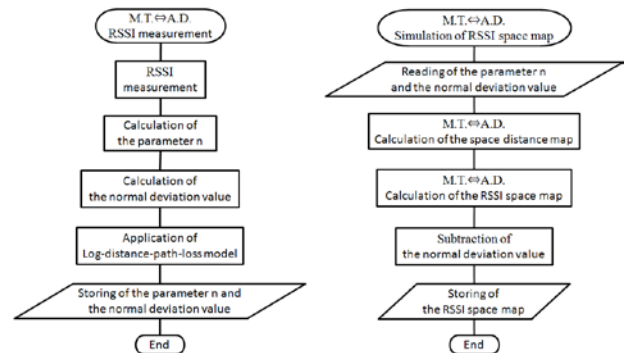
(c) Simulation of the RSSI space map predefined process Fig. 35 (c) shows the flow chart of the space map simulation between the agent device and the mobile terminal. The n parameter and standard deviation are read from the memory of the mobile terminal. Next, the distance to each position in the map of the space, which is used to carry out a simulation, is computed by the mobile terminal. The space map of the RSSI is yielded from the n parameter, the standard deviation

value, and the distance to each position in the map, and the space map is stored in the memory of the mobile terminal. These processes are performed in batches. Once it memorizes what was surveyed, the mobile terminal and the agent device use the map for real-time operation.

  (d) Detection of the LOS predefined process Fig. 35 (d) shows the flow chart of the detection of LOS between the agent device and the cellular phone base station or a GPS satellite. If the transmitter point (such as a base station of a mobile phone) and transmitted signal strength are disclosed, the RSSI is measured between the agent device and a cellular phone base station or a GPS satellite. The RSSI between an agent and transmitter is measured by batch processing only once. Then, the n parameter is calculated using the RSSI by the mobile terminal. Next, the standard deviation for the curve is obtained using actual measurement data and the log-distance path loss model. The n parameter and standard deviation are written and read to and from the memory of the mobile terminal. Next, the distance to each position in the map of the space, which is used to carry out a simulation, is computed by the mobile terminal. The space map of the RSSI is obtained from the n parameter, the standard deviation value, and the distance to each position in the map, and is written to the memory of the mobile terminal. If the transmitter point (such as a base station of the mobile phone) and the transmitted signal strength are not disclosed, window coordinates of the room are detected from the image by rapid object detection. The window coordinates are stored in the memory of the mobile terminal.
(e) Controlling of the agent device predefined process Fig. 35 (d) shows the control flow of the agent device that uses the RSSI space map. The migratory pathway of the agent device is determined from RSSI data obtained at both sides. The RSSI maps of the communication pathway of both the sides of the agent device or the LOS coordinates are read from the memory of the mobile terminal. These RSSI data are compared to the threshold values. An RSSI that is more than the threshold value becomes a candidate target point. (For example, the threshold value that can communicate prepares the restriction beyond -90dBm etc.) The coordinates of the target point are obtained by arbitrating RSSI maps (or LOS coordinates) of both sides of the agent device. The coordinates of the target point are stored in the memory of the mobile terminal. Calculation from the RSSI space maps and storing of target point coordinates in the memory is done via batch processing, and the execution is carried out only once. API is used to control the movement of an agent device in accordance with this course. The flyer-type agent device flies to the target point. Finally, the information communication is performed.
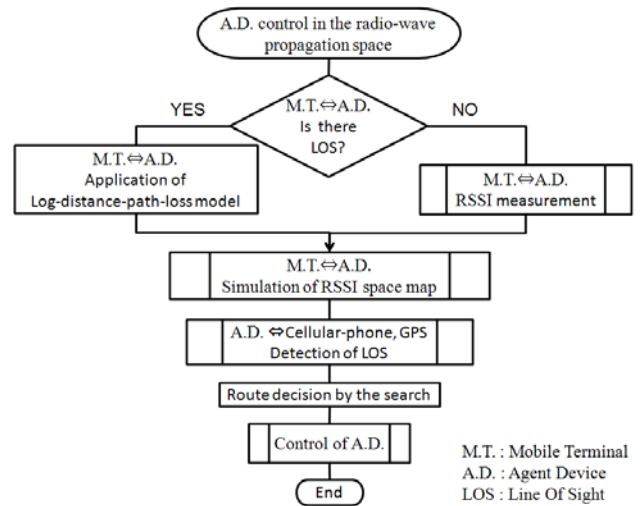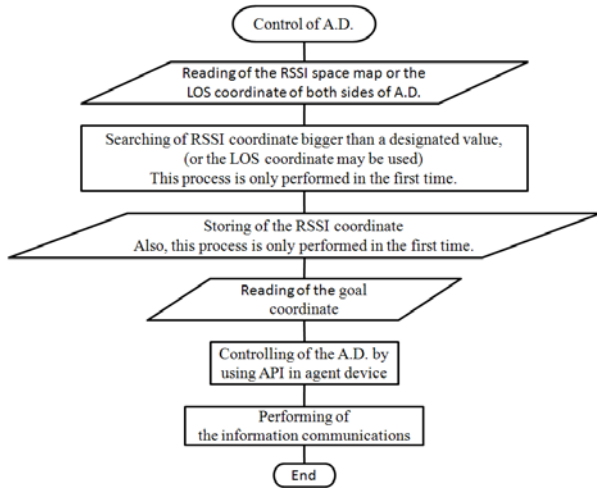

(a) Main flow of the agent device control

(b) RSSI measurement (c) Simulation of the RSSI space map
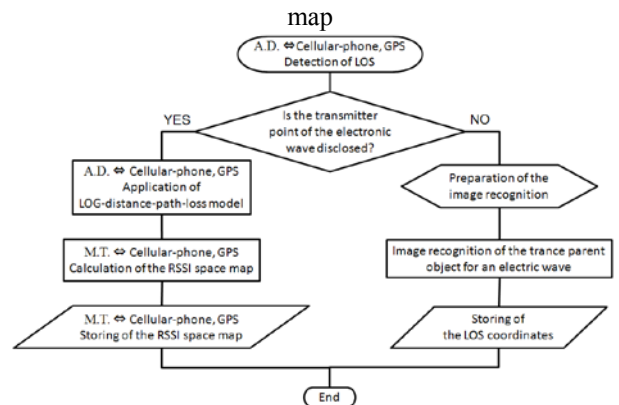
(d) Detection of LOS

(e) Controlling of the agent device

Figure 37: Detailed control flow chart

We show an example of another control method in Fig. 38. First, the mobile terminal measures the RSSIs of all cells. Further, the RSSI is expected to be higher than -90 dBm. The agent device, represented as a transmitter in this case, searches the appropriate RSSI in order to communicate with the receiver. While an agent device in our proposed system may use both a wireless LAN and cellular phone network, it should search for an equal or stronger RSSI position from where it can communicate with the mobile terminal. As shown in Fig. 5, the agent device is equipped with a GPS receiver and/or a mobile Wi-Fi router. As such, an agent device may need to be moved to a nearby window in order to receive a satellite or cellular phone signal. As shown in Fig. 11, there is a window (LOS) near the cell in order to communicate with GPS or cellular phone networks. We assume that the nearby window of the room is the LOS of the radio waves. The window coordinates of the room are detected from the image by rapid object detection. The target cell should satisfy the above-mentioned RSSI conditions. Figure 18 shows the basic method for routing. The route may pass through all the cells in the box having 240 cells. We show the path that passes through a cell by gray circles in Fig. 18. The agent device takes off, and is then aimed at the target cell. It flies according to the program of the mobile terminal toward its goal.
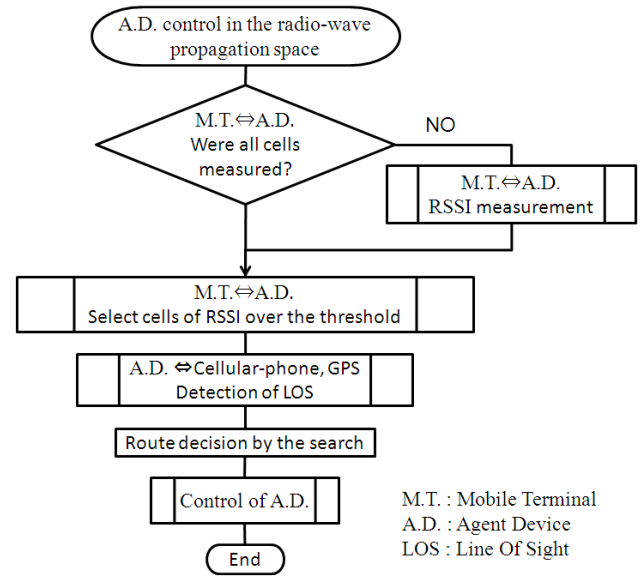

Figure 38: Example of the other control method (Search of all transmitter cells)
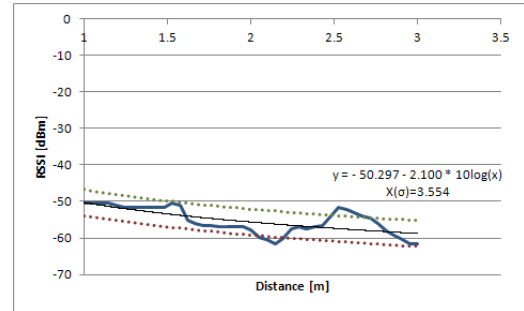

Figure 39: RSSI on a center raw line.
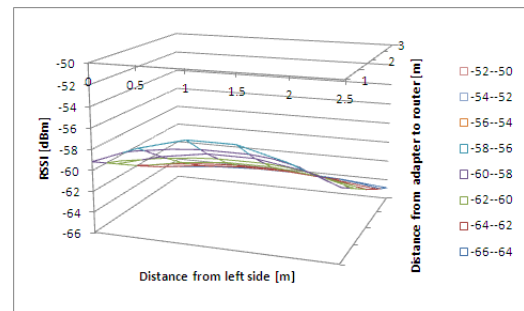
Figure 40: Calculated RSSI map.

We describe in more detail the control sequence. We measured the RSSI on a center raw line in order to approximate to the log-normal path-loss equation. The n and $X(\sigma)$ terms in the equation were derived from the measurement. In this case, n was 2.100 and $X(\sigma)$ was 3.554. We then made a map by using the approximation from the measured data. The map is shown in Fig. 40. The map is displayed on the display of the mobile terminal, as shown in Fig. 41, by the control program. The position of the target was decided from the map. The RSSI of this position should be more than -90 dBm, and the position should be a nearby

window for receiving a GPS signal or cellular phone signal. We assumed that the nearby window of the room is the line-of-sight of the radio waves. The window coordinates of the room were detected from the image by the rapid object detection using Haar-like features [33]. Figure 42 shows the image of the detected object. A goal point was decided from this RSSI map and the coordinates of the window. The cell size is $50cm \times 20cm \times 50cm$ in Fig. 43. We decided to use the dotted line circle as a goal position, as shown in Fig. 43. The RSSI of the goal was -64.213 from RSSI map as shown in Fig. 41. We used Excel and Processing language [34] on the Windows OS for controlling the agent device. The program for controlling the agent device shows the RSSI map in a window. A search of the communication path is then performed. First, the agent device takes off, and is then aimed at the target RSSI value. The trajectory of the device by is shown schematically in Fig. 43. The agent device flew according to the program of the mobile terminal toward this goal. We show the relation of the positions between the mobile terminal and the agent device in Fig. 44. The agent device moved toward this goal after taking off perpendicularly. The flyer-type agent device flew to the target point. The contact sheet of the movie is shown in Fig. 45. Finally, the information communication is performed. In this instance, this flight took approximately $6s$ to arrive at the goal. 87% energy remained after flying using this routing method. The agent device can fly for 12 min. The energy remaining in the agent device after this flight was enough to perform bidirectional communication. The agent device will use more (and potentially all) battery energy if other methods are employed. We show the remaining energy in table 3.

Table 3: Remaining energy after the flight to the goal

	energy
Proposed search method	87%
Search method of all transmitter cells	0%
Dijkstra's Algorithm	0%

This method took approximately $6s$ to arrive at the goal. The time for taking off and going forward was 3 s each. Because RSSI measurement is a batch process in the proposed method, it does not take any additional time. The search method will take approximately $3.3E + 565hr$ to arrive at the goal for all transmitter cells in the worst case. On the other hand, Dijkstra's algorithm will take approximately $1.6hr$ to arrive at the goal in the worst case. The RSSI measurement time was $16.7ms$ in this experiment.

We have summarized these driving times in table 4.

Table 4: Time required for Pocket agent driving

	Time
Proposed search method	$6S$
Search method of all transmitter cells	$3.3E + 565hr$
Dijkstra's Algorithm	$1.6hr$

We could receive position data by using GPS and image data by using the built-in camera. We could then send the message and attached data to an iPad set at a distant place by using Pocket WiFi. We were able to transfer information satisfactorily. The text information (a), house-position information (b), and image of the room (c) are shown in Fig. 46.
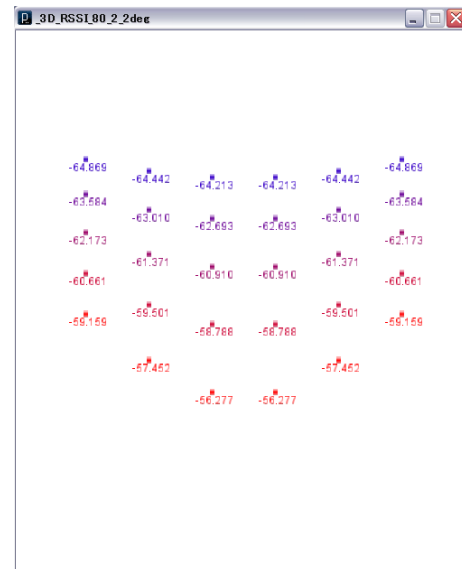
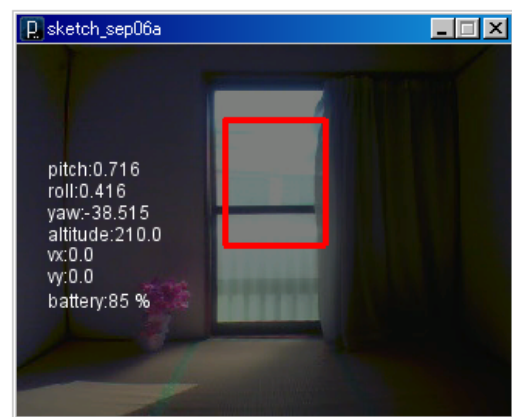

Figure 41: RSSI map in the window.

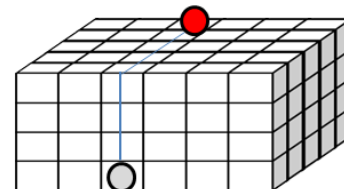Figure 42: Recognition of the window in the room.
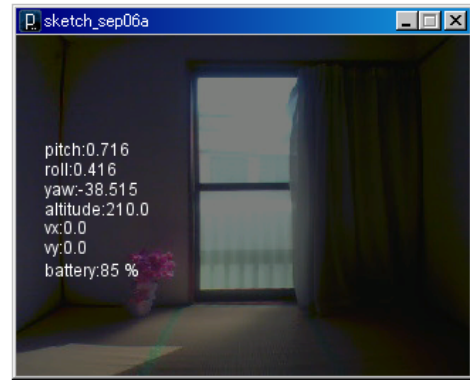

Figure 43: Path and goal position.

Figure 44: Mobile terminal and agent device.

Figure 45:
The contact sheet of the movie of the agent device.

(a)

(b)

(c)

Figure 46: Information from the agent device.
(a): The text information, (b): The house position
information, (c): The image of the room information

5   CONCLUSION

In this study, we proposed various architectures of Pocket agent devices. We then compared these architectures, and summarized their advantages and disadvantages. We conducted experiments at indoor and outdoor locations. First, we simulated RSSI using the log-distance path-loss model. Next, we simulated RSSI using the log-normal path-loss model. These simulated results were compared with the actual measured RSSI. The measured value showed the same tendency as the simulation value. We assumed that the log-normal path-loss model can be used to explore the route for communications. A goal point was decided from this RSSI map and the coordinates of the window. We proposed the direct-routing algorithm by using the log-normal path-loss model and the rapid-object detection using Haar-like features. According to this method, an agent device is able to arrive at the goal in a shorter time than when using other algorithms, thus reducing energy consumption.

For future work, we will research more applications of Pocket agent devices using the direct-routing algorithm.

REFERENCES

[1] M. Weiser, ``The computer for the 21st century,'' ACM SIGMOBILE Mobile Computing and Communications Review - Special issue dedicated to Mark Weiser, Vol.3, Issue 3, pp. 3-11 (1999).

[2] A. S. Tanenbaum, and M. V. Steen, Distributed Systems, Principles and Paradigms, Pearson Education (2003). T. Mizuno, T. Higashino, Y. Miyanishi, K. Suzuki, S. Nishiyama, and F. Satou interpreted to Japanese.

[3] M. F. F. Khan, and K. Sakamura, ``A Review of Technical Solutions to Computational Resource Limitation in Ubiquitous Computing Environment,'' Proceeding of the 2nd International Conference on Pervasive Computing and Applications, 2007 (ICPCA 2007), pp. 472-477 (2007).

[4] Xu Hai-peng, Li Hao, and Li Jia-yin, ``Phase characteristics of a new element for design of a single-layer microstrip reflectarray,'' Proceedings of the 2010

International Symposium on Intelligent Signal Processing and Communication Systems (lSPACS 2010) , pp.1-4 (2010) .

[5] Y. Shibata, Y. Sato, and N. Ogasawara, ``A Disaster Information System by Ballooned Wireless Adhoc Network,'' Proceedings of the International Conference on Complex, Intelligent and Software Intensive Systems, 2009 (CISIS '09), pp. 299-304 (2009).

[6] W. Wang, S. C. Liew, and V. O. K. Li, ``Solutions to Performance Problems in VoIP over 802.11. Wireless LAN,'' IEEE Transactions on Vehicular Technology, Vol. 54, Issue 1, pp. 366-384 (2005).

[7] H. T. Friis, ``A Note on a Simple Transmission Formula,'' Proceedings of the I.R.E. and Waves and Electrons, Vol.34, Issue 5, pp. 254-256 (1946).

[8] J. B. Andersen, T. S. Rappaport, and S. Yoshida, ``Propagation measurements and models for wireless communications channels,'' IEEE Communications Magazine, Vol.52, pp. 42-49 (1995).

[9] T. S. Rappaport, Wireless Communications, Principles & Practices, Prentice Hall (1996).

[10] D. Puccinelli, and M. Haenggi, ``Multipath Fading in Wireless Sensor Networks: Measurements and Interpretation,'' Proceedings of the 2006 IEEE/ACM International Conference on Wireless Communications and Mobile Computing (IWCMC'06), pp. 1039-1044 (2006).

[11] M. K. Awad, K. T. Wong, and Z. bin Li., ``An integrated overview of the open literature's empirical data on the indoor radiowave channel's delay properties,'' IEEE Transactions on Antennas and Propagation, Vol. 56, Issue 6, pp. 1451-1468 (2008).

[12] S. Y. Seidel, and T. S. Rappaport, ``914 MHZ Path Loss Prediction Models for Indoor Wireless Communications in Multifloored Building,'' IEEE Transactions on Antennas and Propagation, Vol. 40, Issue 2, pp. 207-217 (1992).

[13] G. Zhou, T. He, S. Krishnamurthy, and J. A. Stankovic, ``Impact of Radio Irregularity on Wireless Sensor Networks,'' Proceedings of the 2nd international conference on Mobile systems, applications, and services, pp. 125-138 (2004).

[14] M. Hidayab, A. H. Ali, and K. B. A. Azmi, ``Wifi Signal Propagation at 2.4 GHz,'' Proceedings of the Asia Pacific Microwave Conference 2009 (APMC 2009), pp. 528-531, (2009).

[15] J. A. R. P. de Carvalho, H. Veigal, R. Costa, P. A. J. Gomes, and A. D. Reis, ``A Contribution to Experimental Performance Evaluation of Point-to-Point WiMAX Links,'' Proceedings of the IEEE International Symposium on Signal Processing and Information Technology 2008 (ISSPIT 2008), pp. 150-153 (2008).

[16] M. K. Awad, K. T. Wong, and Zheng-bin Li, An Integrated Overview of the Open Literature's Empirical Data on the Indoor Radiowave Channel's Delay Properties,'' IEEE Transactions on Antennas and Propagation, Consumer Device & System, Vol. 56, Issue 5, pp. 1451 - 1468 (2008).

[17] Y. Wang, W. Lu, and H. Zhu, ``Experimental Study on Indoor Channel Model for Wireless Sensor Networks and Internet of Things,'' Proceedings of the 12th IEEE International Conference on Communication Technology (ICCT), 2010, pp. 624-627 (2010).

[18] Y. Chen, and A. Terzis, ``On the Implications of the Log-normal Path Loss Model: An Efficient Method to Deploy and Move Sensor Motes,'' Proceedings of the 9th ACM Conference on Embedded Networked Sensor Systems (SenSys '11), pp. 26-39 (2011).

[19] D. Son, B. Krishnamachari, and J. Heidemann, ``Experimental Study of Concurrent Transmission,'' ACM Trans, Antennas and Propagation (2008).

[20] O. Tekdas, J. H. Lim, A. Terzis, and V. Isler, ``Using Mobile Robots to Harvest Data from Sensor Fields,'' IEEE Wireless Communications Magazine, Vol. 26, pp. 22-28 (2009).

[21] P. Dutta, S. Dawson-Haggerty, Y. Chen, C.-J. M. Liang, and A. Terzis, ``Design and Evaluation of a Versatile and Efficient Receiver-Initiated Link Layer for Low-Power Wireless,'' Technical Report CSD-TR 02-0013, University of California, Los Angeles, Computer Science Department (2003).

[22] O. Yuuki, K. Yamada, T. Mizuno, H. Mineno, and M. Nishigaki, ``Wireless Telecommunication by Using the Sphere Device Wrapped in Adhesives in Blind Zones of Electric Wave,'' Institute of Electronics, Information and Communication Engineers Technical Report, Vol. 112, No. 67, pp. 27-33 (2012).

[23] O. Yuuki, K. Yamada, T. Mizuno, H. Mineno, and M. Nishigaki, Wireless Telecommunication by Using Pocket Agent Device in Blind Zones of Electric Wave, Information Processing Society Trans. Consumer Device & System, Vol.2, No.1, pp. 58-66, (2012).

[24] O. Yuuki, K. Yamada, T. Mizuno, H. Mineno, and M. Nishigaki, ``Wireless Telecommunication by Using a Space Movement Agent Device in Blind Zones of Electric Wave,'' Consumer Device & System IPSJ SIG Technical Report, Vol.2012-CDS-4, No.13, pp. 1-8 (2012).

[25] O. Yuuki, K. Yamada, T. Mizuno, H. Mineno, and M. Nishigaki, ``Wireless Telecommunication by Using the Smart Agent Robot in Blind Zones of Electric Wave,'' Institute of Electronics, Information and Communication Engineers Technical Report, Vol. 112, No. 67, pp. 35-40 (2012).

[26] Transystem Inc. (online), http://www.transystem.com.tw/, November 28, 2011 .

[27] Three.co.uk (online), http://threestore.three.co.uk/broadband/?mifi=1, November 28, 2011.

[28] google map (online), http://maps.google.co.jp/, May 13, 2012.

[29] Pocket WiFi SoftBank C01HW (online), http://mb.softbank.jp/mb/data_com/product/mobilewifi/c01hw/, November 28, 2011.

[30] Eee PC 900A (online), http://www.asus.com/Eee/Eee_PC/Eee_PC_900A/, September 16, 2012.

[31]   inSSIDer   (online),
        http://www.metageek.net/products/inssider/?utm_expid
        =1903281&utm_referrer=http%3A%2F%2Fwww.infra
        expert.com%2Fstudy%2Fwireless23.html,   May   13,
        2012.
[32]   BNR   speed   test   (online)   http://www.musen-
        lan.com/speed/, May 13, 2012.
[33]   Rainer Lienhart and Jochen Maydt, ``An Extended
        Set of Haar-like Features for Rapid Object Detection,''
        Proceedings of the IEEE ICIP 2002, Vol. 1, pp. 900-
        903 (2002).
[34]   processing (online),   http://processing.org/,
        September 13, 2012.

Osamu Yuuki received the B.E. degree from keio University, in 1998. He is currently in the doctoral course in information science in Shizuoka University, Japan. His research interests include distributed computing, and computer networks. He is a member of Information Processing Society of Japan, the institute of electronics, information and Communication Engineers, IEEE.

Kunihiro Yamada received the M.S.degree in electrical engineering from Ritumeikan University,Japan, in 1973, Ph.D.degree in industrial science and engineering from Shizuoka University,2002.In 1973,he joined Mithubishi Electric Corporation,where he was engaged in the design and development of microprocessor.And he was the senior vice president and board director of Renesas Solutions Corporation,2003.He is currently an Professor of Professional Graduate School of Embedded Technology, Tokai University. His research microprocessor structural improvement in the speed and Home network of a mutual complement communication system by wired and wireless. He is a member of IPSJ ,KES International.

Tadanori Mizuno received the B.E. degree in Industrial Engineering from the Nagoya Institute of Technology in 1968 and received the Ph.D. degree in Computer Science in 1987 from the Kyushu University in Fukuoka. In 1968, he joined Mitsubishi Electric Corporation in Kamakura. From 1993 to 2011, he had been a Professor of Informatics at Shizuoka University in Hamamatsu. Since 2011, he is a Professor of Information Science at the Aichi Institute of Technology in Toyota. His research interests include mobile computing, distributed computing, computer

networks, broadcast communication and computing, and protocol engineering. He is a member of Information Processing Society of Japan, the Institute of Electronics, Information and Communication Engineers, IEEE, ACM, and Informatics Society.

Hiroshi Mineno received his B.E. and M.E. degrees from Shizuoka University, Japan in 1997 and 1999, respectively. In 2006, he received the Ph.D. degree in Information Science and Electrical Engineering from Kyushu University, Japan. Between 1999 and 2002 he was a researcher in the NTT Service Integration Laboratories. In 2002, he joined the Department of Computer Science of Shizuoka University as an Assistant Professor. He is now a Asociate Professor at the Graduate School of Science and Technology of Shizuoka University. His research interests include sensor networks as well as heterogeneous network convergence. He is a member of IEEE, ACM, IEICE, IPSJ and Informatics Society.
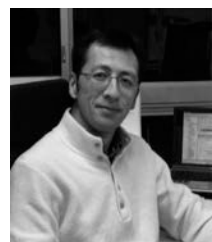
Masakatsu Nishigaki received his Ph.D. in Engineering from Shizuoka University, Japan. He served as a Postdoctoral Research Fellow of the Japan Society for the Promotion of Science in 1995. Since 1996 he has been engaged in research at the Faculty of Infomatics, Shizuoka University. He is now a Professor at the Graduate School of Science and Technology of Shizuoka University. His research interests are in wide variety of information security, especially in humanics security, entertaining security, user authentication, and anti-malware techniques.